Tensile and compressive properties of fresh human carotid atherosclerotic plaques

Eoghan Maher[1], Arthur Creane[2], Sherif Sultan[3,4], Niamh Hynes[3,4], Caitríona Lally[2], Daniel J. Kelly[1]

1. Trinity Centre for Bioengineering, School of Engineering, Trinity College, Dublin, Ireland.
2. School of Mechanical and Manufacturing Engineering, Dublin City University, Dublin, Ireland.
3. Western Vascular Institute, Department of Vascular & Endovascular Surgery, University College Hospital Galway, Ireland.
4. Department of Vascular & Endovascular Surgery, Galway Clinic, Doughiska, Dublin Road, Galway, Ireland.

Corresponding author:

Dr. Daniel Kelly,
Trinity Centre for Bioengineering,
School of Engineering,
Trinity College,
Dublin,
Ireland.

Ph +353-1-8963947 Fax +353-1-6795554
E-mail: kellyd9@tcd.ie

Keywords: Atherosclerotic Plaque, Human, Carotid, Mechanical Properties

Word count: 3509 (Excl abstract and references)

Abstract

Accurate characterisation of the mechanical properties of human atherosclerotic plaque is important for our understanding of the role of vascular mechanics in the development and treatment of atherosclerosis. The majority of previous studies investigating the mechanical properties of human plaque are based on tests of plaque tissue removed following autopsy. This study aims to characterise the mechanical behaviour of fresh human carotid plaques removed during endarterectomy and tested within 2 hours. A total of 50 radial compressive and 17 circumferential tensile uniaxial tests were performed on samples taken from 14 carotid plaques. The clinical classification of each plaque, as determined by duplex ultrasound is also reported. Plaques were classified as calcified, mixed or echolucent. Experimental data indicated that plaques were highly inhomogeneous; with variations seen in the mechanical properties of plaque obtained from individual donors and between donors. The mean behaviour of samples for each classification indicated that calcified plaques had the stiffest response, while echolucent plaques were the least stiff. Results also indicated that there may be a difference in behaviour of samples taken from different anatomical locations (common, internal and external carotid), however the large variability indicates that more testing is needed to reach significant conclusions. This work represents a step towards a better understanding of the *in vivo* mechanical behaviour of human atherosclerotic plaque.

1. Introduction

Myocardial infarction and stroke are acute pathological events that occur during the chronic process of atherosclerosis (Newby, 2005). Rupture or erosion of the artherosclerotic plaque, and the subsequent thrombosis that results in occlusion or embolisation, are the two main mechanisms involved in such conditions (Davies, 2000). While biomechanical forces have been implicated in plaque fatigue and rupture (Cheng et al., 1993; Ku and McCord, 1993; Loree et al., 1992; Richardson et al., 1989), such stimuli are also thought to play a major role in the modelling and remodelling of such plaques (Glagov et al., 1997). Atherosclerotic plaques contain T cells and lipid-laden macrophages (foam cells), which are derived from blood monocytes (Libby, 1995). T cells produce factors which suppress the production of collagen by the smooth muscle cells (SMCs) and stimulate macrophages to produce matrix metalloproteinases (MMPs) which digest the existing collagen and other extracellular matrix components (Nicolaides et al., 2002). The SMCs within the vessel wall, which play a key role in maintaining the structural integrity of the plaque cap (Geng et al., 1997; Seshiah et al., 2002), are influenced by the level of mechanical stretch they experience (Sotoudeh et al., 2002). This may explain why regions of high strain in artherosclerotic plaques correlate with low levels of SMCs (Schaar et al., 2003). These and other studies confirm that vascular tissue mechanics and biology are intrinsically related in the pathogenesis of atherosclerosis.

A complete understanding of the mechanics of diseased arteries is also critical to optimising the outcomes of interventional procedures such as angioplasty and stenting. This has enabled computational tools such as finite element models to be used in the optimization of stent design. Early models focussed on the expansion characteristics of balloon expandable (Chua et al., 2003; Dumoulin and Cochelin, 2000; Etave et al., 2001;

Migliavacca et al., 2002; Petrini et al., 2004; Tan et al., 2001) and self expanding stent designs (Whitcher, 1997). The necessity to understand both lumen gain and vessel injury post-stenting has led to greater interest in modelling stent-plaque-artery interactions (Auricchio et al., 2001; Bedoya et al., 2006; Chua et al., 2004; Early et al., 2009; Lally et al., 2005; Migliavacca et al., 2004; Rogers et al., 1999). Further studies using anisotropic constitutive equations for the artery wall (Holzapfel et al., (2002) have been performed for both stenting (Kiousis et al., 2007) and for angioplasty (Gasser and Holzapfel, 2007). As well as aiding the optimisation of stenting procedures, an increased understanding of the mechanical properties of atherosclerotic tissue might be useful in the planning and optimisation of surgical procedures. For example, prior knowledge of the properties of a carotid plaque could inform the decision on whether to stent or perform an endarterectomy, a surgical procedure to remove atherosclerotic plaque material from an artery by separating the plaque from the arterial wall.

Our understanding of the role of vascular mechanics in all aspects of atherosclerosis, from its development to its treatment, is impeded by insufficient experimental data for diseased human tissue. The majority of experimental investigations of atherosclerotic plaques are performed on cadaveric tissue. Lee et al (1991) dynamically tested the fibrous cap of abdominal aortic plaques in radial compression and related their findings to the cap composition as determined by histology. It was found that hypocellular caps were 1-2 times stiffer than cellular and calcified were 4-5 times as stiff. In a further study Lee et al (1992) performed radial compression relaxation tests on abdominal aortic plaque caps. These results were compared to classifications from intravascular ultrasound imaging and it was found that non-fibrous plaque caps had the lowest static stiffness and longest relaxation time, calcified caps had the highest stiffness and lowest relaxation times

and fibrous caps had values in between the other classifications. In contrast, Loree et al (1994) found no significant difference between the static circumferential tangential moduli of hypocellular, cellular and calcified plaques. Topelski et al (1997) investigated cyclic compressive behaviour in aortoiliac plaques. Three types of plaque behaviour were identified and related to results from histology. Salunke et al (2001) studied the compressive stress relaxation behaviour of aortoiliac plaques when subjected to successive stress relaxation tests and compared the results to histology and to similar tests on healthy vessels. They found that during the loading cycle up to 25% compressive stretch that calcified and fibrous plaques behaved similarly and that both were stiffer than atheromatous plaques. The anisotropic behaviour of diseased iliac arteries was investigated by Holzapfel et al. (2004). Each artery specimen was separated into its different artery and plaque component layers, as determined by high resolution MRI. All the studies mentioned above have been performed on cadaveric material. Given the delay before autopsy, and the fact that there can be changes to soft tissue properties during short term storage (Stemper et al., 2007), there is a need to obtain data for fresh human tissue.

The objective of this study is to determine the mechanical properties of fresh (tested in less than 2 hours) carotid plaques following removal during endarterectomy. For this purpose uniaxial circumferential tension and radial compression tests were performed on plaque samples. This study also investigates in-patient variability and inter-patient variability between specimens and the relationship between plaque properties and their clinical classification and the location of the sample in the carotid bifurcation.

2. Materials and Methods

Tensile and compressive tests were performed on samples taken from plaques of the carotid bifurcation. Plaque specimens were removed from 14 patients (9 men and 5 women, 67±8.84yrs, mean±SD) during routine carotid endarterectomies. All surgeries and tests were performed in the Galway Clinic, Ireland. The study includes 44 compressive and 16 tensile samples obtained from 14 carotid plaques. Table 1 includes all patient and lesion details. Plaque classifications were determined independently by a clinician using routine Duplex ultrasound with grey scale imaging (Nicolaides et al.; Tegos et al., 2001). Ethical approval for testing of the human tissue was obtained.

2.1 Sample Preparation

Plaque specimens were prepared for testing immediately following removal in surgery. Specimens were dissected at the bifurcation, separating them into common, internal and external carotid segments, see figure 1. Each segment was opened by cutting along the axial direction. Circumferential tensile and radial compressive samples were removed from each of the flat rectangular segments using stainless steel punches. Dog-bone shaped tensile samples were used which had a gauge length and width of 4 mm and 1 mm respectively. Regions were deemed suitable for tensile testing if a sample with relatively consistent composition could be obtained within the gauge length of the dog-bone sample. Due to the small diameter of the external carotid, no tensile samples were obtained from these plaque segments. 4 mm diameter compressive samples were also removed from the specimen. Testing samples were allowed to equilibrate in 0.9% saline solution for approximately 30 minutes before measurements of the sample dimensions were recorded.

2.2 Testing Conditions

Testing was performed using a computer controlled, high precision testing device adapted for testing biological specimens (Bose ElectroForce 3100, Bose Corporation, Gillingham, UK). The testing rig has an electromagnetic driven motor, with a stroke resolution of 0.0015 mm, a maximum stroke length of 5mm and a minimum load resolution of 6 mN with the 22N load cell. Screw-based compressive platens and tensile grips were used during testing, and the ability to interchange these allowed the same device to be used for both compressive and tensile testing. All samples were stored in 0.9% saline solution until testing. All samples were tested within two hours of harvesting.

Unconfined compression tests were performed on the 4 mm diameter compressive samples. A sample was placed on the lower platen and the upper platen was moved to apply a small compressive pre-load of 0.01 N to the sample at a crosshead speed of 0.001 mm/s. This ensured a consistent contact between the platen and the top of the sample and minimal strain in the plaque, < 5% in all cases. The sample height was then taken as the distance between the platens at this pre-load. Before testing, preconditioning was achieved by performing 10 loading and unloading cycles to 10% strain at a constant crosshead rate of 1% strain/s. After preconditioning the sample was compressed at the same rate (1%/s) until 60% strain was reached.

For tensile testing, a fast drying permanent marker was used to draw two parallel horizontal lines across the gauge of the samples before testing. The tabs of a dog-bone sample were then clamped in the tensile grips. The tensile grips were lined with sandpaper in order to minimize sample slip within the grips. A tensile preload of 0.01 N was applied to the sample at a rate of 0.001mm/s in order to ensure that the true gauge length was measured. The preload caused only minimal strain in all samples (< 5%). During the tensile

tests strain measurements were taken using a computer based video extensometer. The extensometer automatically recognised marks and edges, and the gauge length after preload and deformation between the gauge marks during testing was recorded by the computer. Before testing the sample thickness was also measured using the video extensometer. Similar preconditioning as with the compressive samples was applied to the tensile sample after which the sample was stretched at a constant rate of 1% strain/s until the maximum stretch allowed by the stroke length of the testing device was reached or until failure occurred in the sample.

2.3 Data Fitting and Analysis

A 2^{nd} order isotropic hyperelastic model (Eqn. 1) was used to fit to the obtained experimental data in this study. A general 2^{nd} order polynomial hyperelastic strain energy function can be defined in terms of the strain invariants as follows (Abaqus Inc):

$$\psi = C_{10}(I_1 - 3) + C_{01}(I_2 - 3) + C_{20}(I_1 - 3)^2 + C_{11}(I_1 - 3)(I_2 - 3) + C_{02}(I_2 - 3)^2 \qquad \text{(Eqn. 1)}$$

where ψ is the strain energy function, C_{ij}, $i + j = 1, 2$ are material constants and I_1 and I_2 are the principle strain invariants. The strain invariants can be expressed in terms of the principle stretches as $I_1 = \lambda_1^2 + \lambda_2^2 + \lambda_3^2$, and $I_2 = \lambda_1^2 \lambda_2^2 + \lambda_1^2 \lambda_3^2 + \lambda_2^2 \lambda_3^2$. For the case of uniaxial testing of an incompressible material the nominal stress is given by:

$$T = \frac{\partial \psi}{\partial \lambda} = 2(1-\lambda^{-3})\left(\lambda \frac{\partial \psi}{\partial I_1} + \frac{\partial \psi}{\partial I_2}\right) \qquad \text{(Eqn.2)}$$

where λ is the stretch in the loading direction. Data fitting was performed using the test data curve fitting function of the finite element package Abaqus 6.7-1, which uses a linear least squares procedure to obtain the constants C_{ij}, $i + j$=1, 2. This method aims to minimize the difference in nominal stress between the experimental test data and the data calculated from Eqn. 2. The relative error, E, between these two values is given by Eqn. 3.

$$E = \sum_i \left[1 - \frac{data\ measured(i)}{data\ calculated(i)}\right]^2 \qquad \text{(Eqn. 3)}$$

It is important to ensure that the constants obtained using this method lead to a stable function. This is done by ensuring that the curves produced are positive definite. Stability checking is done automatically in Abaqus when performing a curve fit. Where an unstable curve is produced the constants are modified to produce a stable response.

As an independent measure of the appropriateness of the fit the root mean square error measure ζ, which is based on the sum of the square error between calculated and measured data, is used (Eqn. 4).

$$\zeta = \frac{\sqrt{\dfrac{\sum_i (data\ measured(i) - data\ calculated(i))^2}{n-q}}}{T_{ref}} \qquad \text{(Eqn. 4)}$$

where n is the number of data points and q is the number of strain-energy function constants. The value T_{ref} is the sum of all nominal stresses for each data point divided by the number of data points.

The compressive data was analysed using a number of different criteria: (1) in-patient variation; (2) inter-patient variation; (3) plaque classification; (4) sample location. However due to the significantly lower number of tensile samples, tensile data was analysed and presented together. All the stress strain data is graphed as nominal stress against nominal strain. As the stress strain curves of the material approach failure the curves, in some cases, become noisy. As a result of this a 10% drop in the stress as the strain increases was viewed as material failure here, and the data wasn't analysed or graphed following such a drop.

3. Results

Significant in-specimen variation in the compressive behaviour of human atherosclerotic plaque was observed, see Fig. 2. For certain specimens, most notably specimens 2, 7 and 9, there is a large amount of variation between samples. However for other specimens (1, 4, and 5) a much lower degree of variation was observed. When comparing the variation seen to the clinical classification there appears to be no direct link between plaque classification and in-specimen variation; for example specimen 4 is a mixed plaque but has low variation while specimen 2 is also mixed but has a higher variability. When plaques were grouped by clinical classification, a large amount of variability in the compressive behaviour for both the calcified and mixed plaque specimens was observed, see Fig. 3. This variability is less evident for the echolucent samples. Comparing the mean curves for each classification

suggested that calcified samples were on average over twice as stiff as the echolucent samples and 1.5-2 times stiffer than the mixed plaque. Large variations are also observed in the compressive properties of samples taken from the same vessel section (either common, internal and external) of the plaque, see Fig. 4. The average curve for each plaque location does suggest some variation, with the common artery being the stiffest and the external the least stiff; however no firm conclusions can yet be made about differences in plaques between the three carotid vessels.

Significant variability was also observed in the tensile properties of fresh human carotid plaque, see Fig. 5. Due to the smaller number of tensile samples, the main conclusion that can be drawn from the tensile data is that there appears to be high variability, both inter-specimen and in-specimen, in the tensile behaviour of these plaques.

The overall mean material constants obtained from curve fitting the compressive and tensile data to a Mooney-Rivlin model are given in Table 2 and 3 respectively. These tables also include information on the mean values for each of the constants obtained from compressive testing for both the samples described by plaque classification and those described by vessel. In the case of tensile data only the overall mean and standard deviation (SD) are reported due to the lower number of samples tested.

4. Discussion

Improved understanding of the mechanical properties of diseased human carotid tissue may enhance our understanding of the pathophysiology of atherosclerosis. Rupture and errosion of such plaques are key mechanisms responsible for the development of cerebrovascular events, which are related to the stress levels within the plaque cap. In this study the entire

plaque is surgically separated from the artery during endarterectomy. This provided an insight into how the plaque as a whole behaved and also enabled comparison to results from ultrasound imaging with grey scale median values (US/GSM). The imaging technique used here differs from previous studies: Lee et al (1992) used intravascular ultrasound imaging; Holzapfel et al (2004) used hrMRI and histology, while numerous other studies have used only histology. The choice of using US/GSM imaging was made as it is a non-invasive imaging technique that is used routinely in the clinic to determine the optimum treatment. This choice of imaging also enabled imaging to be performed before the surgery, which helped reduce the time between plaque removal and completion of sample testing. The plaque was assumed to behave as an isotropic hyperelastic material. The isotropic material assumption was made as tests were only carried out in circumferential tension and in radial compression for the specimens due to the constraint of the size of the plaque specimens. While an anisotropic model has been used for other soft tissues such as artery walls (Holzapfel et al., 2002), the high in-specimen inhomogeneity of the plaques may lead to difficulties in modelling a consistent anisotropic behaviour.

The samples tested in this study generally show a non-linear behaviour during both compressive and tensile testing. The non-linear behaviour of plaque tissue has been demonstrated in previous studies (Salunke et al., 2001; Topelski et al., 1997); the one exception to this nonlinear behaviour known to the authors was reported by Holzapfel et al (2004) who reported that calcified tissue behaves almost linearly elastically. This was in contrast to findings in this study as well as others (Loree et al., 1994; Salunke et al., 2001) which generally found non-linear behaviour when testing tissue classified as calcified. While variability between different plaque specimens has been reported before in the literature (Holzapfel et al., 2004), there appears to be no data available on the in-specimen

variations seen in the specimens in this study. The in-specimen variation observed in this study suggests that much more localised mechanical testing needs to be performed. Correlation of such data with *in vivo* imaging of a higher definition than US/GSM currently provides is also necessary.

The inter-patient variability observed in this study provides further support for patient (or lesion) specific stenting (Pericevic et al., 2009). The high variability between the behaviour of different samples would seem to suggest that one stent design may be better suited to a specific lesion than another; and the fact that there seems to be a relationship between the average behaviour of the artery and the classification from the imaging, it may be possible to use US/GSM to better inform the decision regarding the optimum stent design. As anticipated, calcified plaques are on average stiffer than the other plaque types (Figure 3). This was also reported by Holzapfel et al. (2004), however Salunke et al (2001) found that there was no significant difference between calcified and fibrous plaques. No definitive conclusion could be drawn from our study regarding the anatomical location of the samples (Figure 4). Whilst the average curves seem to indicate that plaque segments in the common carotid are stiffer than in the internal or external; the large variability means that more testing is required in order for a more definitive conclusion to be reached.

There are a few limitations to the analyses performed in this study. The number of samples, particularly with tensile data, limits the conclusions that may be drawn. The main reason for the limited number of tensile samples is that the samples can be relatively large with respect to the total plaque size and given the in-specimen plaque variability the authors had some difficulty in obtaining samples with a relatively consistent material composition within the gauge. While the largest sample size possible was used for these tensile tests, the 4 x 1 mm gauge length may be insufficient to fully prevent edge effects from the clamps.

The tests were also unable to consistently produce failure of the tensile samples, this resulted in not being able to report failure stresses and stretches for this study. However the lack of fresh tissue data as well as the lack of data from human diseased carotid arteries means this data may serve as a basis for constitutive equations used in finite element modelling, with particular relevance to models of carotid lesions. The data can therefore be seen as a basis for predicting outcomes of surgical and interventional procedures using finite element modelling. Once a plaque has been classified *in vivo* the mean values of the hyperelastic constants, as well as the upper and lower bound values of each constant, could be used to predict a range of tissue responses that could be expected for a given procedure or intervention. Whether the large standard deviations reported in this study actually indicates large patient-to-patient variability in plaque properties that needs to be considered in all computational models, or is merely a consequence of significant variability in the properties of any given plaque and the sampling used in this study, needs to be further investigated using more localised testing. This could possibly be achieved using indentation testing (Barrett et al., 2009). Furthermore higher resolution imaging, which has previously been used to detect the presence of stress rising microcalcifications in plaque fibrous caps (Vengrenyuk et al., 2006), could be used to better characterise the heterogeneous nature of plaque material.

In conclusion, this study characterised the radial compressive and circumferential tensile behaviour of fresh carotid atherosclerotic plaques in order to obtain a better understanding of plaque behaviour. The study also aimed to relate these results to imaging which is used clinically to determine if treatment of a lesion is necessary thus giving the results a more applicable clinical significance. It was seen that plaque classifications obtained through US/GSM may be related to the mean behaviour of a lesion. This study

represents a step toward better understanding of carotid plaque behaviour; it's relation to its composition and the further use of finite element modelling in stent design. This data would be important in order to obtain an accurate simulation of interventions such as stent expansion or balloon angioplasty that consider lumen gain, vessel stresses and other factors within the carotid artery. Such simulations could be used clinically to help decide between different treatment options such as stenting and endarterectomy.

Acknowledgments

This material is based upon works supported by the Science Foundation Ireland under Grant No. 07/RFP /ENMF660.

References

AbaqusInc, Mechanical Constitutive Theories Abaqus Theory Manual. Simulia, Abaqus Version 6.7 Documentation.

Auricchio, F., Di Loreto, M., Sacco, E., 2001. Finite-element Analysis of a Stenotic Artery Revascularization Through a Stent Insertion. *Computer Methods in Biomechanics and Biomedical Engineering*, 4, 249-263.

Barrett, S.R., Sutcliffe, M.P., Howarth, S., Li, Z.Y., Gillard, J.H., 2009. Experimental measurement of the mechanical properties of carotid atherothrombotic plaque fibrous cap. *J Biomech*. doi:10.1016/j.jbiomech.2009.04.025.

Bedoya, J., Meyer, C., Timmins, L.H., Moreno, M.R., Moore, J.E., 2006. Effects of Stent Design Parameters on Normal Artery Wall Mechanics. *Journal of Biomechanical Engineering*, 128, 757-765.

Cheng, G.C., Loree, H.M., Kamm, R.D., Fishbein, M.C., Lee, R.T., 1993. Distribution of circumferential stress in ruptured and stable atherosclerotic lesions: A structural analysis with histopathological correlation. *Circulation*, 87, 1179-1187.

Chua, S.N.D., Mac Donald, B.J., Hashmi, M.S.J., 2003. Finite element simulation of stent and balloon interaction. *Journal of Materials Prcessing Technology*, 143-144.

Chua, S.N.D., Mac Donald, B.J., Hashmi, M.S.J., 2004. Effects of varying slotted tube (stent) geometry on its expansion behaviour using finite element method. *Journal of Materials Prcessing Technology*, 155-156, 1764-1771.

Davies, M.J., 2000. The pathophysiology of acute coronary syndromes. *Heart*, 83, 361-366.

Dumoulin, C., Cochelin, B., 2000. Mechanical Behaviour modelling of balloon-expandable stents. *Journal of Biomechanics*, 33, 1461-1470.

Early, M., Lally, C., Prendergast, P.J., Kelly, D.J., 2009. Stresses in peripheral arteries following stent placement: a finite element analysis *Computer Methods in Biomechanics and Biomedical Engineering*, 12, 25-33.

Etave, F., Finet, G., Boivin, G., Boyer, J.-C., Rioufol, G., Thollet, G., 2001. Mechanical properties of coronary stents determined by using finite element analysis. *Journal of Biomechanics*, 34, 1065-1075.

Gasser, T.C., Holzapfel, G.A., 2007. Modeling Plaque Fissuring and Dissection during Balloon Angioplasty Intervention. *Annals of Biomedical Engineering*, 35, 711-723.

Geng, Y.J., Henderson, L.E., Levesque, E.B., Muszynski, M., Libby, P., 1997. Fas is expressed in human atherosclerotic intima and promotes apoptosis of cytokine-primed human vascular smooth muscle cells. *Arteriosclerosis, Thrombosis, and Vascular Biology*, 17, 2200-2208.

Glagov, S., Bassiouny, H.S., Sakaguchi, Y., Goudet, C.A., Vito, R.P., 1997. Mechanical determinants of plaque modeling, remodeling and disruption. *Atherosclerosis*, 131, S13-S14.

Holzapfel, G.A., Sommer, G., Regitnig, P., 2004. Anisotropic Mechanical Properties of Tissue Components in Human Atherosclerotic Plaques. *journal of Biomechanical Engineering*, 126, 657-665.

Holzapfel, G.A., Stadler, M., Schulze-Bauer, C.A.J., 2002. A Layer-Specific Three-Dimensional Model for the Simulation of Balloon Angioplasty using Magnetic Resonance Imaging and Mechanical Testing. *Annals of Biomedical Engineering*, 30, 753-767.

Kiousis, D.E., Gasser, T.C., Holzapfel, G.A., 2007. A Numerical Model to Study the Interaction of Vascular Stents with Human Atherosclerotic Lesions. *Annals of Biomedical Engineering*, 35, 1857-1869.

Ku, D.N., McCord, B.N., 1993. Cyclic stress causes rupture of the atherosclerotic plaque cap. *Circulation*, 88, 1362.

Lally, C., Dolan, F., Prendergast, P.J., 2005. Cardiovascular stent design and vessel stresses:a finite element analysis. *Journal of Biomechanics*, 38, 1574-1581.

Lee, R.T., Grodinsky, A.J., Frank, E.H., 1991. Structure-Dependent Dynamic Mechanical Behavior of Fibrous Caps From Human Atherosclerotic Plaques. *Circulation*, 83, 1764-1770.

Lee, R.T., Richardson, S.G., Loree, H.M., Grodinsky, A.J., Gharib, S.A., Schoen, F.J., Pandian, N., 1992. Prediction of mechanical properties of human atherosclerotic tissue by high-frequency intravascular ultrasound imaging. An in vitro study. *Arteriosclerosis, Thrombosis, and Vascular Biology*, 12, 1-5.

Libby, P., 1995. Molecular bases of the acute coronary syndromes. *Circulation*, 91, 2844-2850.

Loree, H.M., Grodinsky, A.J., Park, S.Y., Gibson, L.J., Lee, R.T., 1994. Static circumferential tangential modulus of human atherosclerotic tissue. *Journal of Biomechanics*, 27, 195-204.

Loree, H.M., Kamm, R.D., Stringfellow, R.G., Lee, R.T., 1992. Effects of fibrous cap thickness on peak circumferential stress in model atherosclerotic vessels. *Circulation Research*, 71, 850-858.

Migliavacca, F., Petrini, L., Colombo, M., Auricchio, F., Pietrabissa, R., 2002. Mechanical behavior of coronary stents investigated through the finite element method. *Journal of Biomechanics*, 35, 803-811.

Migliavacca, F., Petrini, L., Massarotti, P., Schievano, S., Auricchio, F., Dubini, G., 2004. Stainless and shape memory alloy coronary stents: a computational study on the interaction with the vascular wall. *Biomechanics and Modeling in Mechanobiology*, 2, 205-217.

Newby, A.C., 2005. Dual role of matrix metalloproteinases (matrixins) in intimal thickening and atherosclerotic plaque rupture. *Physiological Reviews*, 85, 1-31.

Nicolaides, A.N., Kakkos, S.K., Griffin, M., Geroulakos, G., Bashardi, E., 2002. Ultrasound plaque characterisation, genetic markers and risks. *Pathophysiology of Haemostasis and Thrombosis*, 32, 371-377.

Pericevic, I., Lally, C., Toner, D., Kelly, D.J., 2009. The influence of plaque composition on underlying arterial wall stress during stent expansion: The case for lesion-specific stents. *Medical Engineering and Physics*, doi:10.1016/j.medengphy.2008.11.005.

Petrini, L., Migliavacca, F., Auricchio, F., Dubini, G., 2004. Numerical investigation of the intravascular coronary stent flexibility. *Journal of Biomechanics*, 37, 495-501.

Richardson, P.D., Davies, M.J., Born, G.V.R., 1989. Influence of plaque configuration and stress distribution on fissuring of coronary atherosclerotic plaques. *Lancet*, 2, 941-944.

Rogers, C., Tseng, Y.D., Squire, J.C., Edelman, E.R., 1999. Balloon-Artery Interactions During Stent Placement : A Finite Element Analysis Approach to Pressure, Compliance, and Stent Design as Contributors to Vascular Injury. *Circulation Research*, 84, 378-383.

Salunke, N.V., Topelski, L.D.T., Humphrey, J.D., Mergner, W.J., 2001. Compressive stress-relaxation of human atherosclerotic plaque. *Journal of Biomedical Materials Research*, 35, 17-127.

Schaar, J.A., De Korte, C.L., Mastik, F., Strijder, C., Pasterkamp, G., Boersma, E., Serruys, P.W., Van Der Steen, A.F.W., 2003. Characterizing Vulnerable Plaque Features with Intravascular Elastography. *Circulation*, 108, 2636-2641.

Seshiah, P.N., Kereiakes, D.J., Vasudevan, S.S., Lopes, N., Su, B.Y., Flavahan, N.A., Goldschmidt-Clermont, P.J., 2002. Activated monocytes induce smooth muscle cell death role of macrophage colony-stimulating factor and cell contact. *Circulation*, 105, 174-180.

Sotoudeh, M., Li, Y.S., Yajima, N., Chang, C.C., Tsou, T.C., Wang, Y., Usami, S., Ratcliffe, A., Chien, S., Shyy, J.Y.J., 2002. Induction of apoptosis in vascular smooth muscle cells by mechanical stretch. *American Journal of Physiology - Heart and Circulatory Physiology*, 282.

Stemper, B.D., Yoganandan, N., Stineman, M.R., Gennarelli, T.A., Baisden, J.L., Pintar, F.A., 2007. Mechanics of Fresh, Refrigerated, and Frozen Arterial Tissue. *Journal of Surgical Research*, 139, 236-242.

Tan, L.B., Webb, D.C., Kormi, K., Al-Hassani, S.T.S., 2001. A method for investigating the mechanical properties of intracoronary stents using finite element numerical simulation. *International Journal of Cardiology*, 78, 51-67.

Tegos, T.J., Alomiris, K.J., Sabetai, M.M., Kalodiki, E., Nicolaides, A.N., 2001. Significance of Sonographic Tissue and Surface Characteristics of Carotid Plaques. *American Journal of Neuroradiology*, 22, 1605-1612.

Topelski, L.D.T., Salunke, N.V., Mergner, W.J., 1997. Composition- and history-dependent radial compressive behavior of human atherosclerotic plaque. *Journal of Biomedical Materials Research*, 35, 117-127.

Vengrenyuk, Y., Carlier, S., Xanthos, S., Cardoso, L., Ganatos, P., Virmani, R., Einav, S., Gilchrist, L., Weinbaum, S., 2006. A hypothesis for vulnerable plaque rupture due to stress-induced debonding around cellular microcalcifications in thin fibrous caps. *Proc Natl Acad Sci U S A*, 103, 14678-83.

Whitcher, F.D., 1997. Simulation of in vivo loading conditions of nitonol vascular stent structures. *Computers and Structures*, 64, 1005-1011.

List of Figures and Tables

Table 3: Strain energy constants for tension testing of plaque samples (MPa). M- mixed; Ca - calcified; E - echolucent; C - common carotid; I - internal carotid; Ex - external carotid.

Tables

Table 1: Patient/specimen details

Specimen	Gender	Age, yr	Clinical Classification	No. of Compression Samples	No. of Tensile Samples
1	M	67	Mixed	2 T; 0 C; 2 I; 0 E	0 T
2	M	70	Mixed	5 T; 2 C; 2 I; 1 E	0 T
3	F	72	Mixed	3 T; 0 C; 3 I; 0 E	2 T; 2 C; 0 I
4	F	71	Mixed	4 T; 1 C; 2 I; 1 E	1 T; 1 C; 0 I
5	M	51	Mixed(Lightly calcified) proximal vessel, mostly echolucent at focal plaque	5 T; 3 C; 1 I; 1 E	1 T; 1 C; 0 I
6	M	71	Calcified proximally, mixed distally	4 T; 2 C; 1 I; 1 E	2 T; 0 C; 2 I
7	M	83	Calcified Proximally, mixed distally	7 T; 4 C; 2 I; 1 E	0 T
8	M	73	Calcified Proximally, mixed distally	3 T; 1 C; 1 I; 1 E	1 T; 1C; 0 I
9	F	78	Calcified	8 T; 3 C; 3 I; 2 E	0 T
10	M	65	Mixed	0 T	1 T; 0 C; 1 I
11	M	61	Calcified	1 T; 0 C; 1 I; 0 E	1 T; 1C; 0 I
12	F	63	Mostly calcified, echolucent at origin	0 T	3 T; 3 C; 0 I
13	M	58	Mostly echolucent	2 T; 0 C; 2 I; 0 E	2 T; 2 C; 0 I
14	F	55	Calcified Proximally, mixed distally	0 T	2 T;2 C; 0 I
	Age, mean±SD yr	67±8.84	Total no. of Samples	44 T; 15 C; 20 I; 8 E	16 T; 13 C; 3 I

M, male; F, female; T, total no. of samples for specimen; C, sample from common segment of specimen; I, sample from internal segment of specimen; E, sample from external segment of specimen. Plaque classifications were determined by an independent clinician, who was blinded to the mechanical testing results, based on routine ultrasound with grey scale median imaging.

Table 2: Strain energy constants for compression testing of plaque samples (MPa)

Sample	Classification	Vessel	C10	C01	C20	C11	C02	ζ
1 (i)	M	I	0.042	0	0	0	0	0.0994
1 (ii)	M	I	0.0012	0.0208	0.0004	0	0	0.0971
2 (i)	M	Ex	0.0078	0	0	0	0	0.0996
2 (ii)	M	I	0.004	-0.0009	0	0	0.000546	0.0924
2 (iii)	M	C	0.07	0.041	0.126	0.009	0	0.098
2 (iv)	M	C	0.001468	0.0013	0.00012	0	0.00012	0.0296
2 (v)	M	I	0.001	0.053	0	0	0	0.0958
3 (i)	M	I	0.006	0.04	0.2	0	0	0.0693
3 (ii)	M	I	0.002	0.04	0.08	0	0	0.0992
3 (iii)	M	I	0.005	0.0019	0.0062	0.001	0	0.0883
4 (i)	M	C	0.001	0.00271	0	0	0	0.0894
4 (ii)	M	I	0.00868	0	0	0	0	0.0965
4 (iii)	M	I	0.0012	0	0	0	0	0.0873
4 (iv)	M	Ex	0.001	0.0012	0.0002	0	0	0.0964
5 (i)	E	C	0.0001	0.0164	0.0319	0	0	0.0955
5 (ii)	E	C	0.003	0.004	0.001	0.003	0	0.0955
5 (iii)	M	C	0.002	0.015	0.0195	0	0.001	0.086
5 (iv)	M	I	0.001	0.005	0.042	-0.001	0.0086	0.0952
5 (v)	E	Ex	0.00071	0	0	0	0	0.0985
6 (i)	M	C	0.001	0.00556	0	0	0	0.095
6 (ii)	M	C	0.0005	0.00237	0	0	0	0.0776
6 (iii)	M	Ex	0.001	0.00104	0	0	0	0.0869
6 (iv)	M	I	0.0016	0	0	0	0.00465	0.0283
7 (i)	M	C	0.0001	0	0	0	0.0031	0.0998
7 (ii)	M	C	0.0015	0	0	0	0	0.0858
7 (iii)	Ca	C	0.0001	0	0	0	0.1363	0.0996
7 (iv)	Ca	C	0.005	0.002	0.007	0.001	0	0.0974
7 (v)	Ca	I	0.0102	0	0	0	0	0.0924
7 (vi)	Ca	I	0.001	0.012	0.004	0	0	0.0719
7 (vii)	M	Ex	0.0122	0	0	0	0	0.0998
8(i)	Ca	C	0.001	0.0019	0.1	0.004	0	0.071606
8(ii)	Ca	I	0.001	0.06	0.3	0.004	0	0.036145
8(iii)	Ca	Ex	0.001	0.001	0.1	0.01	0	0.005753
9 (i)	Ca	C	0.001	0.0275	0.1478	0	0	0.0973
9 (ii)	Ca	C	-0.0325	0.106	1.275	0.935	0.1	0.0951
9 (iii)	Ca	I	0.002	0.005	0.12	0	.002	0.0563
9 (iv)	Ca	C	-0.005	0.034	0.0177	0	0	0.0908
9 (v)	Ca	I	0.001	0.0012	0.0059	0	0	0.0637
9 (vi)	Ca	I	0.014	0.0172	0.0948	0.181	0.038	0.0966
9 (vii)	Ca	Ex	0.001	0.001	0.025	0.0085	0	0.071606
9 (viii)	Ca	Ex	0.017	0.04	0.03	0	0	0.036145
11 (i)	Ca	I	0.0005	0	0	0	0.0395	0.005753
13 (i)	E	I	0.001	0.038	0	0	0	0.040922
13(ii)	E	I	0.001	0	0.01	0	0.0011	0.090544
Overall	Mean ± SD		.00449±0.01354	.01357±0.02203	.06238±0.197495	.02626±0.1428	.00761±0.02603	.0828±0.0227
Calcified	Mean ± SD		.001144±0.0106	.0193 ± 0.02929	.1392±0.313344	.07147±0.23459	.01974± 0.04111	.0768±0.0261
Mixed	Mean ± SD		.00753±0.01616	.00999±0.01669	.02063±0.04985	.00039±0.00205	.00078±0.00205	.0866±0.0197
Echolucent	Mean ± SD		.00116±0.00109	.01168±0.01618	.00858±0.013698	.0006±0.001342	.00022±0.00049	.0842±0.0244
Common	Mean ± SD		.00314±0.01978	.01623±0.02729	.10768±0.315057	.0595±0.233479	.01503±0.04080	.0873±0.0173
Internal	Mean ± SD		.00527±0.00941	.01466±0.02011	.04317±0.080941	.00925±0.04044	.00472±0.01183	.0801±0.0226
External	Mean ± SD		0.0052±0.00639	0.0055±0.01394	0.0194±0.034876	0.00231±.0043	0±0	.0801±.03236

M - mixed; Ca - calcified; E - echolucent; C - common carotid; I - internal carotid; Ex - external carotid

Table 3: Strain energy constants for tension testing of plaque samples (MPa)

Sample	Classification	Vessel	C10	C01	C20	C11	C02	ζ
3 (i)	M	C	0.001	0.05	0.06	0.04	0	0.0674
3 (ii)	M	C	0.001	0.35	1.8	0.4	0.621	0.0967
4 (i)	M	C	0.015	0.0051	0.001	0.0006	0.011	0.0988
5 (i)	E	C	0.01	0.01	0.0159	0.09	0	0.0999
6 (i)	Ca	I	0.001	0.185	0.1	0.05	0.09	0.0969
6 (ii)	Ca	I	0.001	0	0.8	1.82	3.32	0.0995
8 (i)	Ca	C	0.1	0	0.2	0	0.106	0.09918
10 (i)	M	I	0.001	0	9.8	0	0	0.0986
11 (i)	Ca	C	0.001	0.01	0.03	0	0.07	0.0998
12 (i)	Ca	C	0.001	0.1	0.275	-0.005	0.27	0.0503
12 (ii)	Ca	C	0.02	0.005	-0.001	0.02	0.155	0.0989
12 (iii)	E	C	0.004	-0.002	-0.005	0.06	0.14	0.0994
13 (i)	E	C	0.02	0.01	0	0.03	0	0.0457
13 (ii)	E	C	0.048	0.069	0	0.061	0	0.0837
14 (i)	Ca	C	0.1	.025	0	0.59	0	0.0547
14 (ii)	Ca	C	0.05	0	0	0.14	0.4	0.0992
Overall	Mean ± SD		0.0234±0.0339	0.0651±0.1061	0.817±2.441	0.206±0.4606	0.324±0.8177	0.0868±0.0201

M - mixed; Ca - calcified; E - echolucent; C - common carotid; I - internal carotid; Ex - external carotid

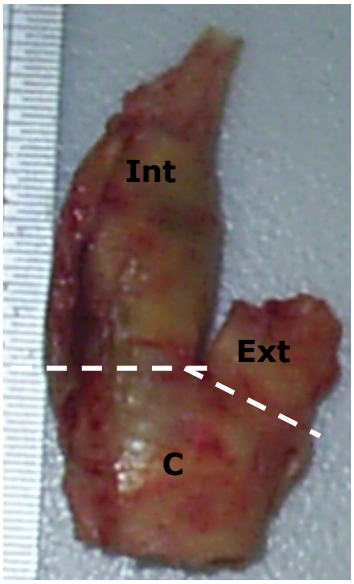
Int
Ext
C

1 Mixed

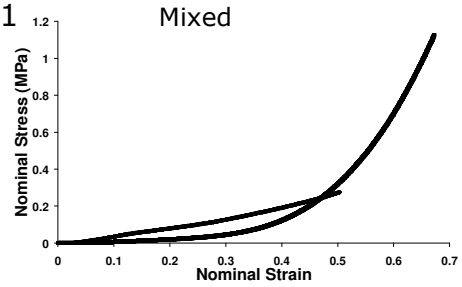

2 Mixed

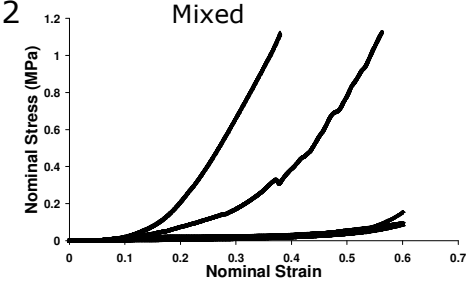

3 Mixed

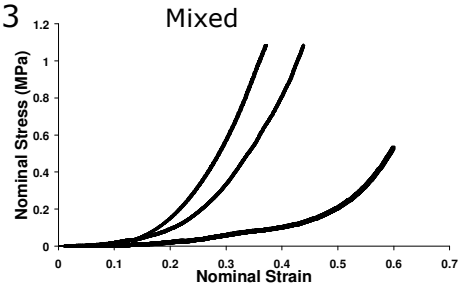

4 Mixed

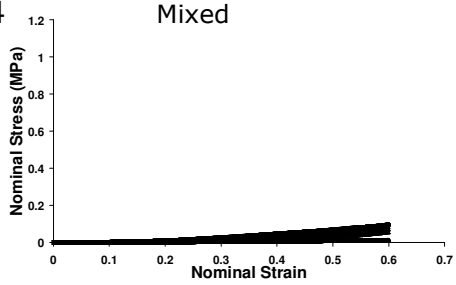

5 Mixed proximally, Echolucent at focal plaque

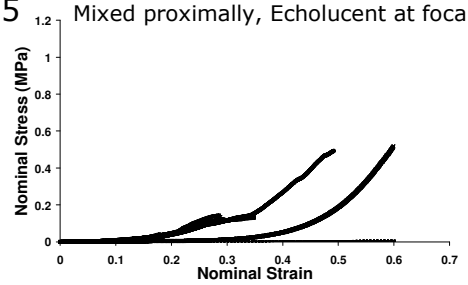

6 Calcified proximally, mixed distally

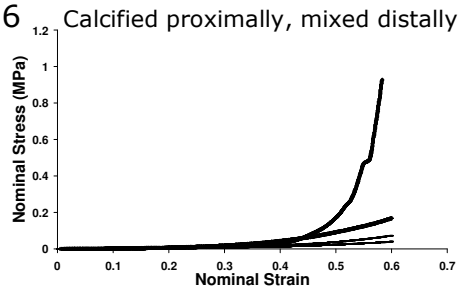

7 Calcified proximally, mixed distally

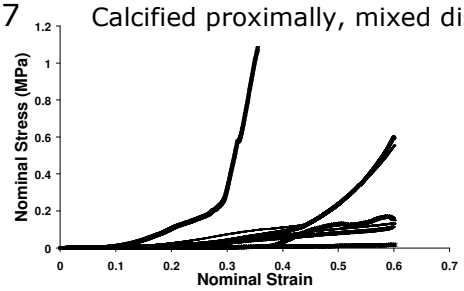

8 Calcified

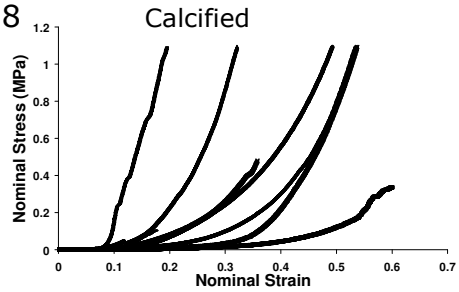

11 Calcified

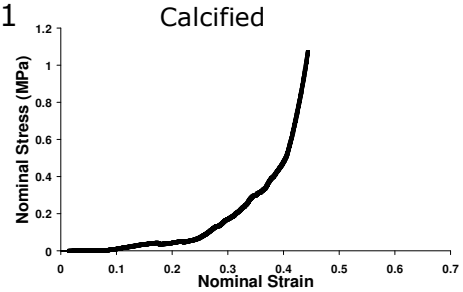

Average

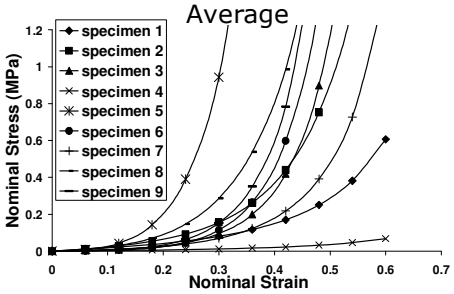

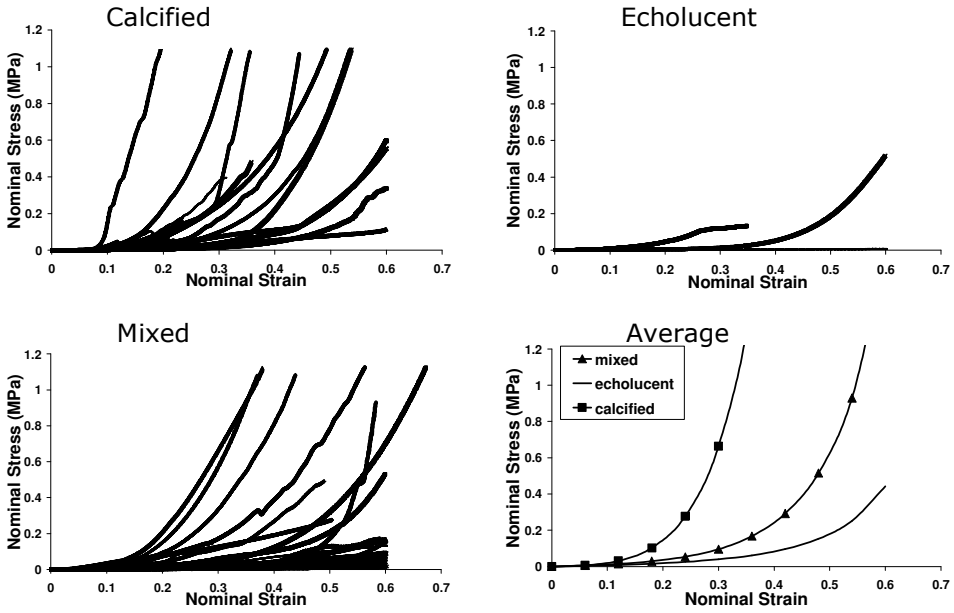
Calcified
Echolucent
Mixed
Average
Nominal Stress (MPa)
Nominal Strain
mixed
echolucent
calcified

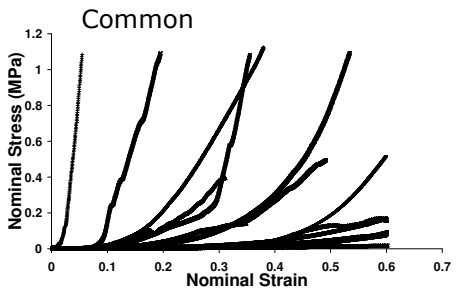
Common
Nominal Stress (MPa)
Nominal Strain
0
0.2
0.4
0.6
0.8
1
1.2
0.1
0.3
0.5
0.7

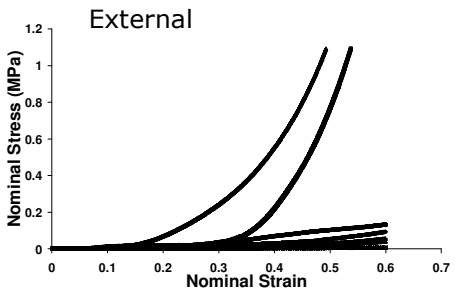
External
Nominal Stress (MPa)
Nominal Strain
0
0.2
0.4
0.6
0.8
1
1.2
0.1
0.3
0.5
0.7

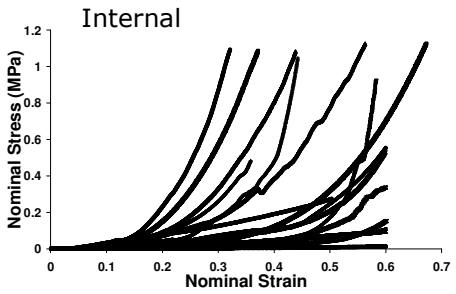
Internal
Nominal Stress (MPa)
Nominal Strain
0
0.2
0.4
0.6
0.8
1
1.2
0.1
0.3
0.5
0.7

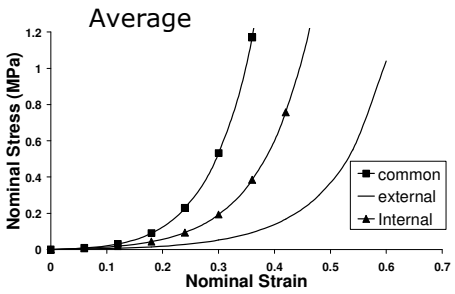
Average
Nominal Stress (MPa)
Nominal Strain
common
external
Internal
0
0.2
0.4
0.6
0.8
1
1.2
0.1
0.3
0.5
0.7

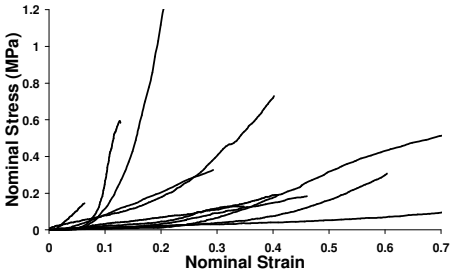
Nominal Stress (MPa)
1.2
1
0.8
0.6
0.4
0.2
0
0
0.1
0.2
0.3
0.4
0.5
0.6
0.7
Nominal Strain